Highlights of the paper:

Risedronate complexes with Mg^{2+}, Zn^{2+}, Pb^{2+}, and Cu^{2+}: species thermodynamics and sequestering ability in $NaCl_{(aq)}$ at different ionic strengths and at T = 298.15 K.

Submitted to *Journal of Molecular Liquids* on July 1st, 2021

Authored by:
Clemente Bretti [a], Concetta De Stefano [a], Paola Cardiano [a], Salvatore Cataldo [b], Alberto Pettignano [b], Giuseppe Arena [c], Carmelo Sgarlata [c], Giuseppa Ida Grasso [c], Gabriele Lando [a,*], Silvio Sammartano [a †]

[a] Dipartimento di Scienze Chimiche, Biologiche, Farmaceutiche ed Ambientali. Università degli Studi di Messina, Viale Ferdinando Stagno d'Alcontres, 31, I-98166 Messina (Vill. S. Agata), Italy.
[b] Dipartimento di Fisica e Chimica – Emilio Segrè, Università di Palermo, Viale delle Scienze, I-90128 Palermo, Italy.
[c] Dipartimento di Scienze Chimiche, Università degli Studi di Catania, Viale A. Doria 6, 95125 Catania, Italy

Correspondence to: Gabriele Lando E-mail: glando@unime.it

- Risedronate interaction thermodynamics with Mg^{2+}, Zn^{2+}, Cu^{2+} and Pb^{2+} is assessed
- Risedronate is a strong chelating agent for the four metal cations reported.
- Entropic change is the main contribution to the stability of the species.
- The highest sequestering ability was found for Cu^{2+} at low pH and ionic strength.
- Risedronate complexes for imaging purposes could be hypothesized.

† Silvio Sammartano passed away on September 27th, 2020. He strongly contributed to the planning of the research, design of the experiments and early discussion of the results. This work is dedicated to his memory, he was a mentor, a colleague, and a friend of all of us.

Submitted to *Journal of Molecular Liquids*

Risedronate complexes with Mg^{2+}, Zn^{2+}, Pb^{2+}, and Cu^{2+}: species thermodynamics and sequestering ability in $NaCl_{(aq)}$ at different ionic strengths and at T = 298.15 K.

Clemente Bretti [a], Concetta De Stefano [a], Paola Cardiano [a], Salvatore Cataldo [b], Alberto Pettignano [b], Giuseppe Arena [c], Carmelo Sgarlata [c], Giuseppa Ida Grasso [c], Gabriele Lando [a,*], Silvio Sammartano [a †]

[a] Dipartimento di Scienze Chimiche, Biologiche, Farmaceutiche ed Ambientali. Università degli Studi di Messina, Viale Ferdinando Stagno d'Alcontres, 31, I-98166 Messina (Vill. S. Agata), Italy.
[b] Dipartimento di Fisica e Chimica – Emilio Segrè, Università di Palermo, Viale delle Scienze, I-90128 Palermo, Italy.
[c] Dipartimento di Scienze Chimiche, Università degli Studi di Catania, Viale A. Doria 6, 95125 Catania, Italy

Correspondence to: Gabriele Lando E-mail: glando@unime.it

ABSTRACT

In this paper, potentiometry and calorimetry were used to determine the thermodynamics of interaction between risedronate and four bivalent metal cations, namely: Mg^{2+}, Zn^{2+}, Pb^{2+}, and Cu^{2+} in aqueous NaCl solutions at different ionic strengths and at T = 298.15 K. The data analysis allowed us to ascertain that the main species formed were the MLH_2, MLH, ML and M_2L; however scarcely soluble species precipitated at acidic pH values, between 4 and 7 depending on the metal cation involved, probably due to the formation of the neutral $M_2L_{(s)}$ species. Comparison of the stability constants with other similar ligands suggests that metal complexation occurs through the phosphonate with an additional stabilizing contribution due to the pyridine moiety. The dissection of the free energy term revealed that the entropic change is the main contribution to the stability of the complexes for all equilibria, except those regarding the formation of the M_2L species, and the main forces involved in these processes are entropic in nature, such as the desolvation of both the ligand and the metal cations. The sequestering ability was evaluated computing the $pL_{0.5}$ parameter at different pH and ionic strength values; the highest ones were found for Cu^{2+} in acidic solutions and at low ionic

† Silvio Sammartano passed away on September 27th, 2020. He strongly contributed to the planning of the research, design of the experiments and early discussion of the results. This work is dedicated to his memory, he was a mentor, a colleague, and a friend of all of us.

strength, whereas $pL_{0.5}$ values for both Pb^{2+} and Zn^{2+} were slightly lower. Results reported in this work may be helpful in the assessment of the use of risedronate as effective chelating agent and for understanding the mechanism of action of this molecule as a drug.

Keywords: risedronic acid; potentiometry; calorimetry; solution thermodynamics; sequestering ability

1. Introduction

Bisphosphonates (BPs) (e.g., alendronate, risedronate, and ibandronate), a class of compounds widely used in medicine as antiresorptive drugs for the treatment of bone disorders such as Paget disease, osteoporosis, hypercalcemia and bone metastasis [1-4], are known to help maintaining bone mass, to inhibit osteoclast-mediated bone resorption as well as to reduce the risk of both vertebral and non-vertebral fractures [5, 6], although some cases of atypical femoral fractures (AFF) have been reported in Asian women with prolonged bisphosphonate exposure [7]. The clinical efficacy of BPs is mainly based on two key properties, i.e. their capacity to strongly bind to bone hydroxyapatite crystals [8, 9] and their inhibitory effects on osteoclast precursors and mature osteoclasts [10]. Among BPs, both alendronate and risedronate have been found to be efficient drugs for the treatment of osteoporosis and Paget's disease having similar effect when evaluating mineral/matrix ratio, yet alendronate turns out to be more effective than risedronate as to its relative proteoglycan content, mineral maturity/crystallinity, and pyr/divalent collagen cross-link ratio [11]. Risedronate has also been reported to help preserving bone microarchitecture in breast cancer survivors [12] and that some diphosphonate salts may be employed in bone imaging [13].

Risedronic acid (Figure 1) is characterized by a P-C-P bridge bound to a pyridine ring in the β position; it is a derivative of pyrophosphate where the carbon atom replaces the oxygen of the P-O-P bridge, thus making the molecule neither chemically nor enzymatically hydrolyzable. Information about solvate structures of risedronic acid were provided by Brüning et al. [14].

Fig.1 Structure of risedronic acid

Malavasi et al. [15] observed that risedronate can modulate positively osteoblast differentiation. In addition, the above authors evidence that risedronate may be also incorporated on the surface of dental implants thanks to its anabolic effects on osteoblasts. Interaction of risedronate with nanoapatite has also been studied via FTIR, Raman and solid NMR spectroscopies [16]; it has been suggested that risedronate adsorption on apatitic supports corresponds to an ion substitution reaction with phosphate ions at the crystal surface. The interaction of risedronate with bone mineral hydroxyapatite was studied by Mukherjee et al. [17] and Ironside et al. [18] with somehow different conclusions. The mechanism of hydroxyapatite crystals growth inhibition is believed to result from the complexation of calcium by bisphosphonates, that would take place *via* the bidentate chelation of deprotonated oxygens present on hydroxyapatite surface, due to the similarity of the O-O and the Ca-O bond distance [3]. Solid state interaction between alendronate and different metal cations was studied by Deacon et al. [19].

As to the inhibitory effect of osteoclasts by bisphosphonate-based drugs, so far two hypotheses have been proposed that are linked to the presence of nitrogen within the molecule backbone. Nitrogen lacking bisphosphonates (*e.g.*, etidronate and clodronate) can be metabolically incorporated into non-hydrolyzable ATP analogues, which interfere with ATP-dependent cellular pathways, whilst nitrogen-containing bisphosphonates inhibit farnesil pyrophosphate synthase (FPPS), the key enzyme involved in the biosynthesis of mevalonate/cholesterol, thus suggesting that nitrogen plays a crucial role in osteoclast inhibition. Accordingly, Hounslow et al. [20] hypothesize that the bisphosphonate protonated nitrogen may act as an analogue of the carbocation in the transition state of the enzymatic reaction. In this context, a detailed characterization of the interaction of risedronate with both the proton and some selected metal cations may significantly help to understand and predict the efficacy and bioavailability of risedronate in complex matrixes. Interaction of risedronate with metal cations is poorly investigated. According to some indications, the oral assumption with water containing high levels of calcium and/or magnesium inhibits risedronate absorption [21]; yet a robust thermodynamic study aimed at clarifying the chemico-physical phenomena occurring between metal cations and risedronate in water is still missing. A review about complexing ability of biphosphonates, excluding risedronate, was recently published by Matczak and co-workers [22]; the authors report that the stability of Mg^{2+} complexes is sizably larger than that of the Ca^{2+} homologous species, in line with Foti et al. findings for etidronic acid [23].

Here we report on the interactions between risedronate and some selected metal cations (*i.e.*, Mg^{2+}, Cu^{2+}, Pb^{2+}, Zn^{2+}) to ascertain whether the presence of metals lowers risedronate bioavailability, which might have adverse effects on the efficacy of therapy. To this end, potentiometric and calorimetric

investigations in aqueous solution have been carried out to have a detailed description of the complexes formed by risedronate with Mg^{2+}, Ca^{2+}, Cu^{2+}, Pb^{2+} or Zn^{2+}.

2. Materials and methods

2.1 Chemicals

The chemicals employed as well as their purity are reported in Table 1. Risedronic acid solutions were prepared by weighing risedronic acid monohydrate, 99%, supplied by HEHUI CHEMICAL CO., LIMITED, P.R. China. The resulting concentrations were checked potentiometrically by alkalimetric titrations. Hydrochloric acid (HCl), and sodium hydroxide (NaOH) aqueous solutions were prepared by diluting concentrated stock solutions (ampoules from Sigma Aldrich), and standardized against sodium carbonate and potassium hydrogen phthalate, respectively, previously dried in an oven at $T = 383.15 \pm 0.1$ K for two hours. Sodium chloride was dried in an oven at $T = 383.15$ K for at least 2 hours before weighing. $CaCl_2 \cdot 2H_2O$, $MgCl_2 \cdot 6H_2O$, $ZnCl_2$, $CuCl_2 \cdot 2H_2O$ and $Pb(NO_3)_2$ aqueous solutions were standardized against EDTA standard solutions. All solutions were prepared with analytical grade water ($\rho = 18$ MΩ·cm) using grade A glassware.

Table 1. Description of the chemical used (all purchased from Sigma-Aldrich). Purity (mass) as stated by the supplier.

Chemical	CAS n°	Purity (% wt.)
Sodium chloride	7647-14-5	≥ 99 %
Sodium hydroxide	1310-73-2	≥ 99 %
Hydrochloric acid	7647-01-0	≥ 99 %
Potassium phthalate monobasic	877-24-7	≥ 99.5 %
Sodium carbonate	497-19-8	≥ 99.5 %
Risedronic acid monohydrate	105462-24-6	99 %
Magnesium chloride hexahydrate	7791-18-6	≥ 99 %
Zinc chloride anhydrous	7646-85-7	≥ 98 %
Copper chloride dihydrate	10125-13-0	≥ 99 %
Lead nitrate anhydrous	10099-74-8	99 %

2.2 Apparatus and procedure for potentiometric measurements

The speciation of the M^{2+} – Ris systems was obtained by ISE-H^+ potentiometric titrations carried out using two apparatuses. The first equipment (University of Palermo) consisted of a model 654 Metrohm potentiometer, equipped with a combined glass electrode (Orion, Ross type 8102) and a Model 665 Metrohm motorized burette; the second apparatus (University of Messina) consisted of a Metrohm 809 Titrando equipped with an automatic burette (total volume 10 cm^3) and a combined glass electrode (Metrohm, model 6.0262.100). The estimated accuracy for both systems was ± 0.2 mV and ± 0.003 mL for e.m.f. and titrant volume readings, respectively. The apparatuses were connected to a PC and controlled by a suitable homemade computer program (apparatus A) or Tiamo 2.5 software (Metrohm, apparatus B) to control titrant delivery, data acquisition and to check for e.m.f. stability. All titrations were carried out under magnetic stirring; presaturated N_2 was bubbled through the solution to exclude/prevent O_2 and CO_2 dissolution. For each measurement 25 cm^3 of titrand solution containing suitable amount of risedronic acid ($0.5 \leq c_L$ / mmol $dm^{-3} \leq 3.0$), metal cation ($0.5 \leq c_M$ / mmol $dm^{-3} \leq 2.0$, generally, $c_M \leq c_L$) $HCl_{(aq)}$ and $NaCl_{(aq)}$ was added to reach pre-established values of pH (~ 2.0) and ionic strengths ($0.1 \leq I$ / mol $dm^{-3} \leq 1.0$) and the titrand solutions were titrated with CO_2-free standard sodium hydroxide solutions up to pH ~ 10.0 or until the electrode started drifting towards lower pH values which indicated the onset of precipitation of sparingly soluble species that are hardly detectable by the naked eye in the initial state. Potentiometric measurements were performed at T = 298.15 K, whose value were maintained constant using circulating water from a thermocryostat (model D1-G Haake). Further details on the potentiometric measurements are reported in Table 2.

Table 2. Experimental conditions of M^{2+} - Ris^{4-} potentiometric titrations.

I/ mol L^{-1}	Metal cation	$C_M{}^{2+a}$	$C_{H4Ris}{}^a$	c_M:c_L	pH range	titrations
0.010 - 1.694	Mg^{2+}	0.9 - 2.2	0.9 - 2.1	0.49 – 1.07	2.80 - 8.53	36
0.097 - 1.004	Cu^{2+}	0.8 – 1.9	1.3 - 1.9	0.42 – 1.54	2.22 - 4.00	12
0.097 - 0.966	Zn^{2+}	1.0 - 1.7	1.5 - 2.1	0.48 – 0.67	2.50 - 5.31	14
0.097 - 0.715	Pb^{2+}	0.5 – 0.6	1.2 - 1.5	0.33 – 0.51	2.91 - 7.51	14

[a] mmol L^{-1}.

2.3 Apparatus and procedure for calorimetric measurements

Isothermal titration calorimetry experiments were carried out using two nano-ITC calorimeters (TA Instruments) equipped with a reference and a sample cell (active volume: 0.943 or 0.988 cm^3), following the procedure recommended by Sgarlata et al. [24]. Measurements were run in the overfilled mode which does not require any correction for liquid evaporation and/or for the presence

of the vapor phase. All titrations were carried out at T = 298.15 K using a 0.250 cm^3 syringe with a stirring rate of 250 rpm. The reference cell was always filled with ultra-pure water (R = 18 MΩ cm). All solutions were degassed under vacuum for about 15 minutes before starting the experiments to eliminate air bubbles. The power curves were integrated through NanoAnalyze, a software supplied by TA Instruments able to obtain the gross heat released/absorbed in the reaction. The calorimeter was calibrated chemically by a test $HCl_{(aq)}$/$TRIS_{(aq)}$ reaction according to the procedure described [18]. The instrument was also checked through electrical calibration.

For the determination of the M^{2+}/Ris^{4-} complex formation enthalpies, the sample cell was filled with a $H_4(Ris)_{(aq)}$ solution ($0.3 \leq c_L$/mmol $dm^{-3} \leq 2$) and sodium hydroxide to neutralize the desirable number of protons whilst the syringe with the proper metal cation solution ($0.5 \leq c_M$/mmol $dm^{-3} \leq 20$). Measurements were also carried out by titrating solutions of $H_4(Ris)_{(aq)}$ ($1.8 \leq c_L$/mmol $dm^{-3} \leq 2.0$) into solutions of Cu^{2+} or Zn^{2+} ($0.5 \leq c_M$/mmol $dm^{-3} \leq 1.0$). $NaCl_{(aq)}$ was added in equal amount both in the syringe and in the cell. At least three titrations were carried out for each system at each ionic strength value. Heats of dilution were determined in different (blank) experiments by titrating solutions of either the proper metal ion or $H_4(Ris)_{(aq)}$ into a solution containing $NaCl_{(aq)}$ only.

2.4 Calculations

ESAB2M [25] was used to refine all the parameters of the acid-base potentiometric titrations (E^0, K_w, liquid junction potential coefficient, j_a, and analytical concentration of reagents) whereas BSTAC [26] was employed for the calculation of equilibrium constants. The non-linear least square computer program LIANA was used to fit different equations [26]. Calorimetric titrations were analyzed with HypCal, a general-purpose computer program for the determination of standard reaction enthalpy and binding constant values by means of calorimetric data. Parameters were determined by simultaneously analyzing data from different titrations [27].

All equilibria described in this paper are expressed by the following equations:

$$j\,M^{n+} + H_iL^{(i-4)} = M_jH_iL^{(i+jn-4)} \qquad K_i \qquad (1)$$

or

$$j\,M^{n+} + i\,H^{+} + L^{4-} = M_jH_iL^{(i+jn-4)} \qquad \beta_i \qquad (2)$$

where M, H and L are the metal ion of interest, the proton and the risedronate anion (Ris^{4-}), respectively. Distribution diagrams were obtained by using HySS [28]. Throughout the paper,

uncertainties are given as 95 % confidence interval. The conversion from the molar to the molal concentration scale was performed using the appropriate density values [29].

The ionic strength dependence of the equilibrium constants was studied in this work by means of the extended Debye-Hückel equation (EDH) and the SIT (Specific ion Interaction Theory) [30-34] model. Considering a generic complex formation constant, expressed as in eq. (2), the equilibrium constants as a function of the activity coefficients may be expressed by eq. (3):

$$\log \beta_{ji} = \log \beta^0_{ji} + j \cdot \log \gamma_{M^{n+}} + i \cdot \log \gamma_{H^+} + \log \gamma_{L^{4-}} - \log \gamma_{MjH_iL^{(i+jn-4)}} \quad (3)$$

both models assume that the variation of the activity coefficients with ionic strength can be expressed by the general formula

$$\log \gamma = -z^2 \cdot 0.51 \cdot I^{0.5}/(1+1.5 \cdot I^{0.5}) + f(I) \quad (4)$$

which according to eq. (3) becomes:

$$\log \beta_{ji} = \log \beta^0_{ji} - 0.51 \cdot z^* \cdot \text{D.H.} + f(I) \quad (5)$$

$$\text{D.H.} = \frac{\sqrt{I}}{1 + 1.5 \cdot \sqrt{I}} \quad (5a)$$

$$z^* = \Sigma\,(\text{charge})^2_{\text{reactant}} - \Sigma\,(\text{charge})^2_{\text{product}} \quad (5b)$$

where $\log \beta^0_{ji}$ is the equilibrium constant at infinite dilution and $f(I)$ is a term accounting for the ionic strength dependence. The differences between the two models stems from the adopted concentration scale (molar and molal for the EDH equation and the SIT model, respectively) as well as from the nature of the $f(I)$ term:

$$\log \beta_{ji} = \log \beta^0_{ji} - 0.51 \cdot z^* \cdot \text{D.H.} + C_{ji} \cdot I_c \quad \text{EDH approach} \quad (6)$$

$$\log \beta_{ji} = \log \beta^0_{ji} - 0.51 \cdot z^* \cdot \text{D.H.} + \Delta\varepsilon_{ji} \cdot I_m \quad \text{SIT approach} \quad (7)$$

In the SIT model, $\Delta\varepsilon_{ji}$ is the combination of the specific interaction coefficients of the species involved in the equilibrium and the ions of the supporting electrolyte. For example, in the case of eq. (3) in $NaCl_{(aq)}$, it is:

$$\Delta\varepsilon_{ji} = j \cdot \varepsilon(M^{n+}, Cl^-) + i \cdot \varepsilon(H^+, Cl^-) + \varepsilon(Na^+, L^{4-}) - \varepsilon(Na^+, M_jH_iL^{(i+jn-4)}) \quad (8)$$

When a neutral species, such as the M_2L species for a divalent metal cation, is involved, eq. (8) becomes:

$$\Delta\varepsilon_{20} = 2 \cdot \varepsilon(M^{2+}, Cl^-) + \varepsilon(Na^+, L^{4-}) - k_m(M_2L) \quad (8a)$$

where k_m is the Setschenow coefficient.

2.5 Sequestering ability

The sequestering ability of risedronate towards the metal cations is computed by resorting to $pL_{0.5}$. This semi-empirical parameter allows for the comparison among ligands as it eliminates from the formation constants of a given M/L system the contribution of specific protonation constant of the ligand, the hydrolysis constants of the metal cation and any other reaction that competes with that under analysis (e.g., chloride complexes); in addition $pL_{0.5}$ does not depend on the speciation scheme, but only on the experimental conditions (pH, ionic strength and temperature) used for its computation. Briefly, a Boltzmann type equation (see eq. (9)) is used to model molar fraction (χ_M) of the metal cation, present in trace concentration ($c_M = 10^{-14}$ mol dm^{-3} in this work), complexed to the ligand vs. the antilog of the ligand analytical concentration. A fit of the points calculated at different pL values provides the sigmoids, the pL value corresponding to $\chi_M = 0.5$ readily provides $pL_{0.5}$. The higher the value of this parameter the better the sequestering ability of the ligand in the chosen condition

$$\chi_M = \left[\frac{1}{1+10^{(pL-pL_{0.5})}}\right] \quad (9)$$

The reader may find further details as to $pL_{0.5}$ definition and use in [35, 36].

3. Results and discussion

All potentiometric titrations run for the M^{2+}/Ris^{4-} systems were refined simultaneously, exploiting an ad hoc feature of BSTAC4. Risedronate protonation constants were taken from our previous work

[37-39]. Hydrolysis constants of the metal cations and the stability constants of metal chloride species for Mg^{2+}, Zn^{2+}, Cu^{2+} and Pb^{2+} were taken from refs [40, 41], respectively; however, these species are not relevant, due to the relatively narrow pH range investigated. By following such a procedure, a set of equilibrium constants at infinite dilution as well as the ionic strength dependence parameter (EDH model (eq. (6)) are obtained. The results for all the metal cations are reported in Table 3. M_2L and MH_iL (with $0 < i < 2$) are the main species for all systems, though the prevailing species depend on the specific metal cation considered. The formation of scarcely soluble species was detected with all metal ions; noteworthy, the formation of such species occurred at pH values which were much lower than expected and, surprisingly, independent of the metal cation employed. Anyway, the unexpectedly low pH at which precipitation occurred is not compatible with the formation of $M(OH)_{2(s)}$; preliminary test performed with XRF indicated that the solid phase is M_2L, but systematic measurements are still in progress. The isolation of M_2(BP) solids has been reported for Pb^{2+} and Cd^{2+} interaction with 1-hydroxyethane-1,1-diphosphonic acid (etidronic acid, HEDP) [22]. For the sake of information, in some cases (e.g., for Pb^{2+} and Cu^{2+}), the solid dissolved at pH > 10 (*i.e.*, beyond the pH of interest) and, accordingly, these data points were excluded from the data analysis. The neutral MLH_2 was detected for all the metal ions investigated while MLH was not found for Cu^{2+}. The investigated metal ions formed the mononuclear species (ML) with the exception of Zn^{2+}; the dinuclear (neutral) M_2L species was formed by Cu^{2+}, Mg^{2+} and Zn^{2+} whereas it was not detected for Pb^{2+}. Polynuclear species such as the $M_3L_2H_2$ and $M_4L_3H_3$ were reported for similar molecules by Matczak-Jon in previous work [42] these species as well as other with different number of protons (and combination thereof) were tested but models invariably failed to converge. The speciation schemes are similar for the four the metal cations; however, the pH range that could be explored was narrow owing to precipitation, and this likely explains why we did not obtain the same set of species for the four metal ions. In fact, whereas for Mg^{2+}, Cu^{2+} and Zn^{2+} measurements were carried out in the presence of an excess, though little, of the specific metal cation, experiments for Pb^{2+} could not be carried out up to the same pH value due to occurrence of precipitation at very acidic pH values. Some runs pointed to the existence of Pb_2L; however, the parameters (standard deviation and mean deviation) taken as a criterion for convergence/goodness of fit, exceed the limit set to include a species and were thus rejected. The value for such a species is reported in parenthesis (Table 3) and has to be regarded as a tentative value; the same applies to the values shown for CuHL and ZnL.

As to the values of the ionic strength dependence parameter (C), the metal cations which show a greater tendency to form chloride species (Cu^{2+} and Pb^{2+}), are characterized by a higher value compared to Zn^{2+} and Mg^{2+}. This could suggest that at high ionic strength, the presence of high chloride concentration helps the stabilization of the Cu^{2+}/*Ris* and Pb^{2+}/*Ris* systems, with possible

formation of ternary complex species. Mean deviations were 1.3, 0.94, 2.1, and 2.1 mV for Mg^{2+}, Cu^{2+}, Zn^{2+}, and Pb^{2+}, respectively. Noteworthy, no significant systematic deviations were observed which makes us confident as to lack of artifacts.

The stability for the ML^{2-} species at I = 0.1 mol dm^{-3} follows the order:

Cu^{2+} (14.2) > Zn^{2+} (13.3, guessed values) > Pb^{2+} (9.4) > Ca^{2+} (6.3, [37]) ~ Mg^{2+} (6.1) Risedronate

This is quite common and reproduces the trend observed for similar bisphosphonates such as etidronic acid [43], in which a methyl group replaces the 3-(methylene)pyridine moiety.

Cu^{2+} (12.1) > Zn^{2+} (10.5) > Mg^{2+} (6.3) ~ Ca^{2+} (6.1) Etidronate

The larger stability of the ML species formed by Cu^{2+}, Zn^{2+}, Pb^{2+} indicates that the pyridinic nitrogen is involved in the M(*Ris*) species of these metal ions whilst the similarity of the values for the ML species obtained for the interaction of Mg^{2+} and Ca^{2+} with risedronate and etidronate leads to conclude that the pyridinic moiety is not bound in the two alkaline-earth complexes. The larger stability is likely to be ascribed to nitrogen electron-withdrawing effect rather than to its chelating ability. Fang et al. [44] reported on the solid/liquid interaction of a hydroxyapatite-derivatized zoledronate with Pb^{2+} and Cu^{2+} concluding that the interaction occurs through the oxygen atoms rather than the amino group of imidazole. Even though zoledronate imidazole and risedronate pyridine groups have different basicity and complexing ability, Feng's conclusion might be extended to risedronate; however, this deserves specific spectroscopic measurements. Noteworthy, Matczak-Jon [22] reported that the nitrogen atom was involved into the ternary complexation of a bisphosphonate for iminodimethylenediphosphonic interaction with Pt^{2+} at pH ~ 1 and for Zn^{2+} at pH values greater than 7, whereas other metal cations such as Mg^{2+}, Ca^{2+}, Ni^{2+}, Co^{2+} and Mg^{2+} involved phosphonate coordination only. In the present case, precipitation occurs well before the amino group may be deprotonated; thus, the coordination of nitrogen would then result from the deprotonation of the amino group triggered by the complexation of the metal ion, which seems highly unlikely.

Comparisons of the metal complex formation constants of risedronate and etidronate with pyrophosphate (PP) reveal that the equilibrium constants of the formers are always much higher than the latter ones. For the above ligands, the stability trend of the five ML species is quite similar, even though for PP the formation constant value of the PbL species is much closer to those of the CuL and ZnL compared to risedronate and etidronate. Therefore, the presence of a carbon atom as a spacer instead of an oxygen seems to display a stabilizing effect on the metal complexes.

Table 3. Results obtained from the analysis of the potentiometric titrations with BSTAC4 at T = 298.15 K and at p = 0.1 MPa. Data in parenthesis are estimated (see text).

Equilibrium	log β^0	C	pH range
$Mg^{2+} + L^{4-} + 2H^+ = MgLH_2^0$	23.00 ± 0.01 [a]	0.37 ± 0.01 [a]	2 - 8
$Mg^{2+} + L^{4-} + H^+ = MgLH^-$	16.50 ± 0.01	-0.41 ± 0.02	2 – 8
$Mg^{2+} + L^{4-} = MgL^{2-}$	7.84 ± 0.02	0.56 ± 0.01	2 – 8
$2Mg^{2+} + L^{4-} = Mg_2L^0$	12.28 ±0.02	-0.22 ± 0.05	2 – 8
$Cu^{2+} + L^{4-} + 2H^+ = CuLH_2^0$	24.52 ± 0.02 [a]	2.43 ± 0.02 [a]	2 – 4
$Cu^{2+} + L^{4-} + H^+ = CuLH^-$	(19.42)	(2.1)	
$Cu^{2+} + L^{4-} = CuL^{2-}$	15.81 ± 0.02	1.56 ± 0.04	2 – 4
$2Cu^{2+} + L^{4-} = Cu_2L^0$	19.85 ±0.02	2.99 ± 0.04	2 – 4
$Zn^{2+} + L^{4-} + 2H^+ = ZnLH_2^0$	25.11 ± 0.13 [a]	-0.62 ± 0.15 [a]	2 – 5
$Zn^{2+} + L^{4-} + H^+ = ZnLH^-$	20.30 ± 0.11	-0.56 ± 0.14	2 – 5
$Zn^{2+} + L^{4-} = ZnL^{2-}$	(15.3)	(-2.8)	
$2Zn^{2+} + L^{4-} = Zn_2L^0$	18.63 ±0.24	-0.45 ± 0.11	2 – 5
$Pb^{2+} + L^{4-} + 2H^+ = PbLH_2^0$	25.94 ± 0.01	1.66 ± 0.06	2 – 7
$Pb^{2+} + L^{4-} + H^+ = PbLH^-$	19.12 ± 0.02	2.51 ± 0.10	2 – 7
$Pb^{2+} + L^{4-} = PbL^{2-}$	10.95 ± 0.03	2.52 ± 0.16	2 – 7
$2Pb^{2+} + L^{4-} = Pb_2L^0$	(15.8)	(4.1)	-

[a] 95 % C.I.

Since the thermodynamic details of the complexation equilibria do not directly emerge by the Gibbs free energy term alone, the separation of the ΔG^0 term into the enthalpic and entropic components may allow to unveil the driving forces of the processes occurring in solution, such as specific interactions between the metal ion and risedronate functional groups as well as metal and/or ligand desolvation upon complexation. Calorimetric titrations were carried out to directly collect the heat of formation of the complex species thus providing a complete thermodynamic characterization of the M^{2+}/*Ris* equilibria. Some examples of typical calorimetric titrations are shown in Figure 1.

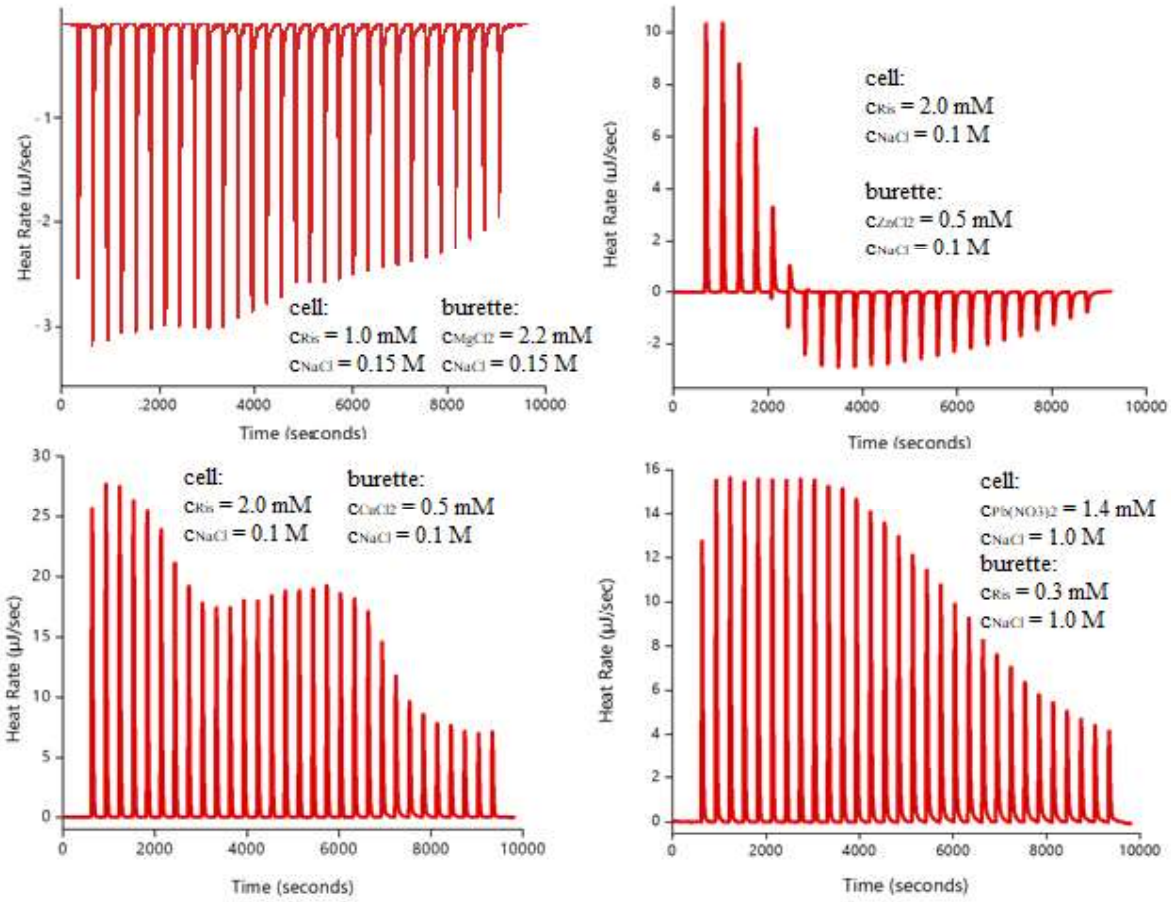

Figure 1. Example of calorimetric titrations carried out on the M^{2+}/*Ris* systems at $T = 298.15$ K.

Results obtained from the analysis of the calorimetric titration data are listed in Table 4. The thermodynamic parameters are expressed for each species in terms of both the stepwise (eq. (1), except for Zn_2L) and overall (eq. (2)) equilibria.

The formation of the MLH_2 species with Zn^{2+} is always entropically favored and driven resulting from metal and ligand desolvation, regardless of the ionic strength value. At I = 0.1 mol dm^{-3}, a favorable enthalpic contribution is also found. The formation of the M_2L complex is enthalpy favored and driven in all cases. Similar features are observed in the case of the Mg^{2+} complexes whose formation is always driven by entropy (with a negative ΔH^0 value for MLH_2 as in the case of Zn^{2+} at the lowest I value) except for the M_2L species. The enthalpic drive for these dinuclear species may be attributed to the favorable attractive interactions between the ligand and the metal ions which also cause a loss of degrees of freedom of the resulting complex as indicated by the unfavorable entropic term.

The overall parameters for Cu^{2+} reveal that the formation of the complexes is both enthalpy and entropy favored regardless of the ionic strength; however, interesting insights may emerge from the

stepwise values. In particular, the formation of MLH_2 and ML species is entropy driven at lower ionic strength values while the enthalpic term largely prevails (MLH_2) or is comparable (ML) to the entropic contribution to ΔG^0 at 1.0 mol dm^{-3}. M_2L complex formation is always driven by enthalpically favorable interactions (with a negative or slightly positive ΔS^0 value) as observed for the other metal ions.

The formation of all Pb^{2+} complex species is entropy favored and driven (except for MLH_2 at the lowest *I* value) and may be ascribed to desolvation and orientation disorder of the hydration water molecules upon complexation. A favorable enthalpic contribution (which is even comparable to that of ΔS^0 in the case of MLH_2 at 1.0 mol dm^{-3}) is found for the formation of the protonated complex species.

Table 4. Thermodynamic parameters [a] for the complex formation of Mg^{2+}, Zn^{2+}, Cu^{2+} and Pb^{2+} with risedronate at different ionic strength, $T = 298.15$ K and $p = 0.1$ MPa.

			Stepwise [b]			Overall [c]		
M^{2+}	I [d]	species	$-\Delta G^0$	ΔH^0	$T\Delta S^0$	$-\Delta G^0$	ΔH^0	$T\Delta S^0$
Mg^{2+}	0.15	MLH_2	14.4	-3.4	11.1	115.7	-17.5 (7) [e]	98.2
	0.15	MLH	17.0	26.3	43.2	79.4	31.2 (7)	110.6
	0.15	ML	33.7	27.1	60.8	33.7	27.1 (9)	60.8
	0.15	M_2L	18.9	-21.1	-2.2	52.6	6 (3)	58.6
Zn^{2+}	0.1	MLH_2	26.8	-5.9	20.9	129.2	-18.7 (7)	110.5
		M_2L	91.1	-93.0	-1.9	91.1	-93 (2)	-1.9
	0.5	MLH_2	21.9	41.8	63.7	119.6	21.1 (8)	140.7
		M_2L	81.1	-108.3	-27.2	81.1	-108.3 (8)	-27.2
	1.0	MLH_2	18.2	44.3	62.5	114.2	16 (3)	130.2
		M_2L	75.8	-136.0	-60.2	75.8	-136 (2)	-60.2
Cu^{2+}	0.1	MLH_2	25.2	2.8	28.0	127.6	-10 (4)	117.6
		ML	81.1	-21.3	59.8	81.1	-21.3 (7)	59.8
		M_2L	18.9	-17.7	1.2	100.0	-39 (3)	61.0
	0.5	MLH_2	27.2	5.7	32.9	124.9	-15 (7)	109.9
		ML	78.7	-10.7	68.0	78.7	-10.7 (4)	68.0
		M_2L	19.2	-27.3	-8.1	97.9	-38 (4)	59.9
	1.0	MLH_2	32.2	-32.7	-0.5	128.2	-61 (5)	67.2

		ML	80.5	-39.7	40.8	80.5	-39.7 (8)	40.8
		M_2L	21.9	-17.3	4.6	102.4	-57 (6)	45.4
Pb^{2+}	0.1	MLH_2	32.8	-17.0	15.9	135.3	-29.8 (6)	105.5
		MLH	34.9	-7.0	28.0	98.1	-1.0 (6)	97.1
		ML	53.8	59.0	112.8	53.8	59 (4)	112.8
	0.5	MLH_2	33.1	-14.3	18.8	130.8	-35.0 (4)	95.8
		MLH	36.2	-15.1	21.1	96.3	-16.0 (6)	80.3
		ML	52.9	42.0	94.9	52.9	42 (4)	94.9
	1.0	MLH_2	35.9	-10.5	25.4	131.9	-38.8 (6)	93.1
		MLH	41.4	-7.8	33.6	100.2	-16.0 (7)	84.2
		ML	56.7	14.0	70.7	56.7	14 (5)	70.7

[a] in kJ mol^{-1}; [b] according to eq. (1), except for Zn_2L, [c] according to eq. (2); [d] $NaCl_{(aq)}$, in mol dm^{-3}; [e] errors on the last significant figure are given in parentheses.

The complex formation constants of M^{2+}/*Ris* complexes were calculated at I = 0.1, 0.5 and 1.0 mol dm^{-3} by means of eq. (6) and using the data reported in Table 3. The $pL_{0.5}$ parameter was calculated at different pH, temperature and ionic strength values as described in the section 2.5.

A graphical comparison of the $pL_{0.5}$ values obtained at different pH values and at different ionic strength values for the four metal cations as well as for Ca^{2+} is given in Figure 2.

Data reported in pH ranges in which the precipitation of scarcely soluble species was observed are reported as dashed lines. The speciation model used to obtain $pL_{0.5}$ values includes the estimated equilibrium constants (ZnL, Pb_2L and CuHL). It has to be emphasized that only ZnL exclusion/inclusion is found to be relevant to $pL_{0.5}$ values and therefore even the dashed data reported in Figure 2 maintain their validity over the entire pH range except for zinc.

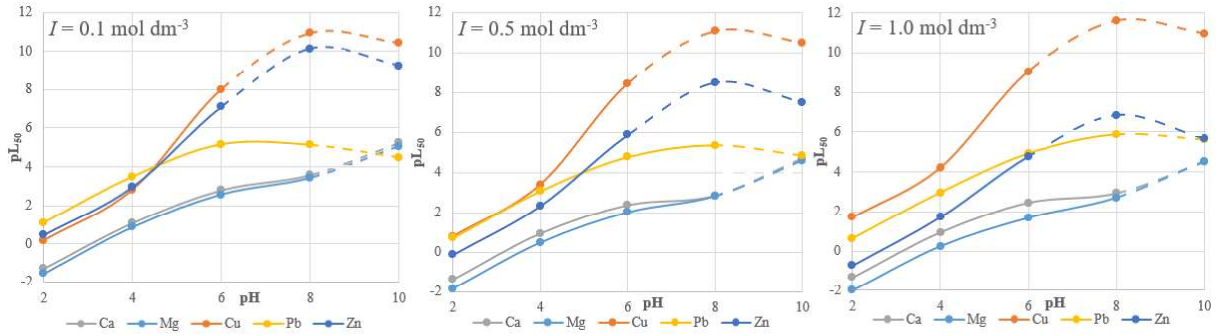

Figure 2. $pL_{0.5}$ values determined at different pH and ionic strength values and at $T = 298.15$ K and at $p = 0.1$ MPa. Lines (solid and dashed) are connectors, not the result of a fitting procedure. Dashed lines refer to pH ranges in which the formation of scarcely soluble species was observed.

From Figure 2 it can be stated that the sequestering ability of risedronic acid increases with increasing pH up to pH ~ 8; at pH > 8 the hydrolysis of Pb^{2+}, Zn^{2+} and Cu^{2+} competes with risedronate complexation. Ionic strength only influences the $pL_{0.5}$ for Zn^{2+} with a fairly strong negative effect, as also suggested by the negative C (see Table 3). Broadly speaking, risedronate sequestering ability is highest for Cu^{2+}, though in acidic solutions and at low ionic strength, $pL_{0.5}$ values for both Pb^{2+} and Zn^{2+} are slightly higher than those for Cu^{2+}. Moreover, as a result of the higher tendency of Pb^{2+} to undergo hydrolysis, Pb^{2+} $pL_{0.5}$ values are higher than those for Zn^{2+} in acidic solutions, whilst the opposite is true in neutral and basic solution. $pL_{0.5}$ values for Ca^{2+} and Mg^{2+} are very similar over the entire pH range and conditions examined; interestingly, the $pL_{0.5}$ at pH ~ 10 is always similar for the three mentioned metal cations, although the stability constants of CaL and MgL are significantly lower than that for PbL.

Compared to other ligands, Ca^{2+}, Mg^{2+}, Zn^{2+}, and Cu^{2+} $pL_{0.5}$ values for risedronate are lower than the ones found for methylglycindiacetic acid (MGDA, [45]) at pH < 6, whereas are higher than those of MGDA at higher pH values. The $pL_{0.5}$ values reported for Zn^{2+}, Cu^{2+}, and Pb^{2+} and phytic acid (Phy, [46]) at $I = 0.15$ mol dm^{-3} roughly reproduce the picture obtained for MGDA except for Pb^{2+}, for which phytic acid is a better sequestering ligand over the whole pH range. In principle this suggests that risedronate might be exploited to chelate target metal cations in different experimental conditions, especially at pH > 6.0.

Complex formation constants in the molar concentration scale calculated from data in Table 3 were converted to the molal concentration scale according to the procedure outlined in the experimental section. The data reported for the Ca^{2+}/Ris^{4-} complex formation constants [37] were also converted and then fitted to the SIT model (eqs. (7-8a)) to obtain the specific interaction coefficients of complex species; those for the interaction of H^+ and Cl^-, Ris^{4-} and Na^+, as well as those of metal cations and chloride have been taken from literature. Known as well as refined specific interaction coefficients

are listed in Table 5. For neutral species, the Setschenow (eq. (8a)) rather than the specific interaction coefficients were refined. The specific interaction coefficients of the guessed species (CuHL, Pb_2L and ZnL) should be regarded as tentative.

Table 5. Specific interaction coefficients of Eqs. 8-8a for the Mg^{2+}, Cu^{2+}, Pb^{2+}, and Zn^{2+}/Ris^{4-} system at T = 298.15 K and at p = 0.1 MPa.

x	y	ε(x,y)	Ref
H^+	Cl^-	0.125	[47]
Na^+	L^{4-}	-0.155	[39]
Mg^{2+}	Cl^-	0.302 - 0.353 · log m_{NaCl}	[40]
Ca^{2+}	Cl^-	0.183 - 0.243 · log m_{NaCl}	[40]
Cu^{2+}	Cl^-	0.11	[32]
Zn^{2+}	Cl^-	-0.20	[32]
Pb^{2+}	Cl^-	0.16	[32]
k_m (CaH_2L)		-0.32±0.01	This work
Na^+	$CaHL^-$	-0.26±0.01	This work
Na^+	CaL^{2-}	-0.10±0.01	This work
k_m (Ca_2L)		0.44±0.02	This work
k_m (MgH_2L)		0.07±0.01	This work
Na^+	$MgHL^-$	0.71±0.01	This work
Na^+	MgL^{2-}	-0.37±0.01	This work
k_m (Mg_2L)		0.74±0.02	This work
k_m (CuH_2L)		-2.17±0.03	This work
Na^+	$CuHL^-$	-1.98±0.03	This work
Na^+	CuL^{2-}	-1.58±0.03	This work
k_m (Cu_2L)		-2.88±0.04	This work
k_m (PbH_2L)		-1.73±0.03	This work
Na^+	$PbHL^-$	-2.70±0.03	This work
Na^+	PbL^{2-}	-2.84±0.03	This work
k_m (Pb_2L)		-4.57±0.04	This work
k_m (ZnH_2L)		0.87±0.01	This work
Na^+	$ZnHL^-$	0.68±0.01	This work
Na^+	ZnL^{2-}	2.75±0.04	This work
k_m (Zn_2L)		0.60±0.01	This work

[a] u_r (ε, relative standard uncertainty on the parameter ε). Standard uncertainties: $u(T)$ = 0.1 K

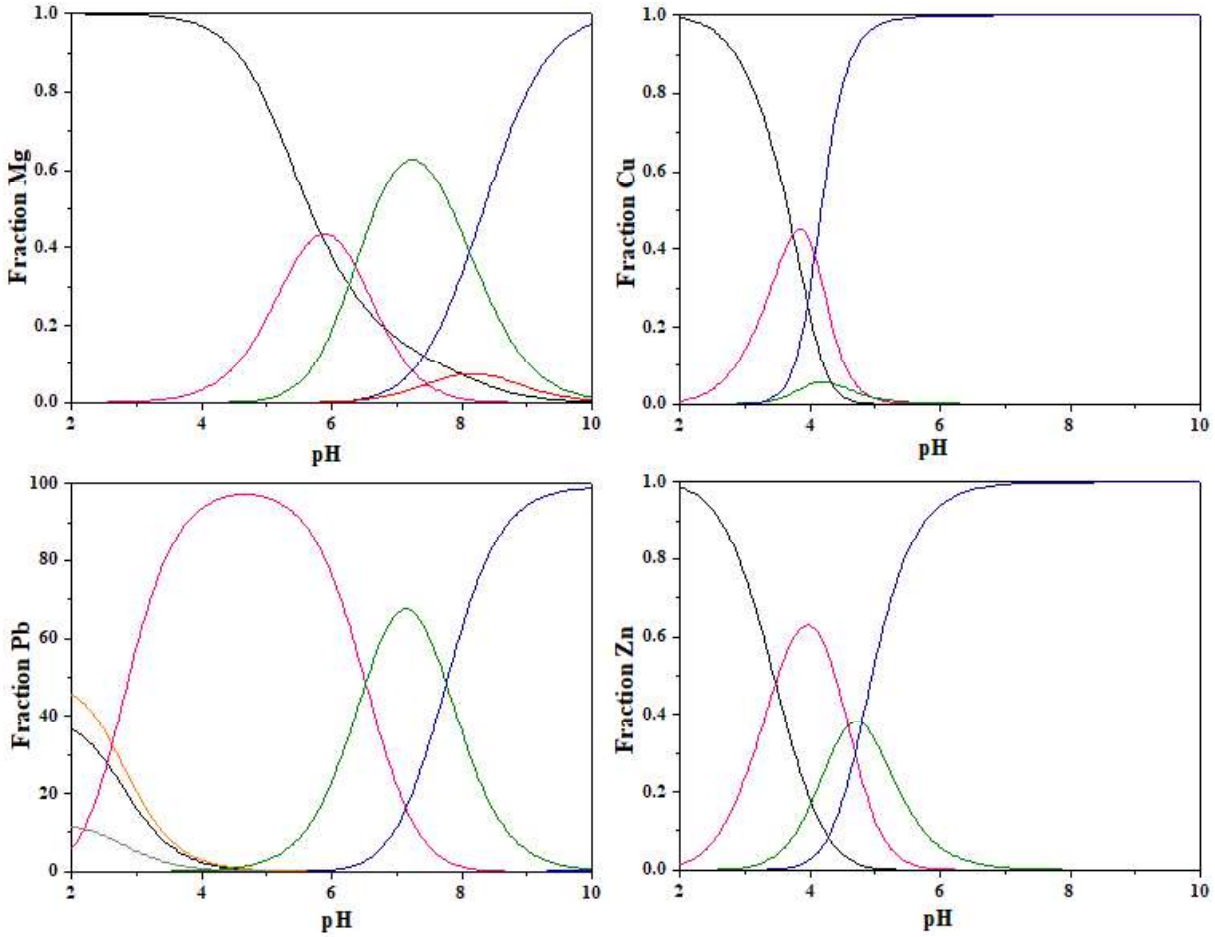

Figure 3 Risedronate distribution diagrams at T = 298.15 K and I = 0.15 mol dm^{-3}. C_{Ris}= 0.005 mol dm^{-3} and C_M = 10^{-6} mol dm^{-3} for all metal cations except for Mg^{2+} (10^{-3} mol dm^{-3}); risedronate concentration roughly reproduces the concentration resulting from the dissolution of a tablet of risedronate drug in the volume of a glass (100 cm^3). Species: M^{2+} (black line), MLH_2 (pink), MLH (green), ML (blue), M_2L (red), MCl (orange), MCl_2 (gray).

The distribution diagrams reported in Figure 3 show that even though the stoichiometry of the species is the same for all the metal cations, their relevance changes with conditions. As an example, the pH at which the M_2L species reaches the maximum formation percentage is ~ 4.0, ~ 4.5, ~ 7.7 and ~ 8.2 for Cu^{2+}, Zn^{2+}, Pb^{2+} and Mg^{2+}, respectively. Analogously, the metal:ligand concentration ratio above which the formation of the M_2L becomes significant is 1:33, 1:2, 1:2 and 1:40 for Cu^{2+}, Zn^{2+}, Pb^{2+} and Mg^{2+}, respectively (calculations not reported). Moreover, the relative importance of the species in the distribution diagrams is very different, for Zn^{2+} and Cu^{2+} the ML is the most important species yet at acidic pH values, whereas for Mg^{2+} and Pb^{2+} this applies only at pH > 8. At physiological pH value, pH = 7.4, the species distribution are as follows:

Table 6. Species formation percentages in the conditions of Figure 3 at the physiological pH = 7.4.

Species	M = Mg	M = Cu	M = Pb	M = Zn
Free M^{2+}	12	-	-	-
MLH_2	6	-	8	-
MLH	62	-	64	-
ML	12	100	30	100
M_2L	4	-	-	-

Conclusions

The present study shows that risedronate is a strong chelating agent for the four metal cations here reported. Although previous literature findings on similar systems (*e.g.*, BPs) suggest that complexation occurs mainly through the coordination of the phosphonate groups, the comparison of the present data with those of similar ligands having bisphosphonate groups only indicates that risedronate pyridine moiety further contributes to the stability of the complexes.

Calorimetric data allowed to unveil the often opposing entropic and enthalpic contributions to the overall complexation processes in solution. The formation of the mononuclear complex species was found to be favored and driven by entropy mostly due to ligand and metal ion desolvation upon complexation. A favorable enthalpic contribution was also observed depending on the ionic strength or the protonation degree of the complexes. Conversely, the M_2L species (when formed) was always driven by enthalpy due to multiple attractive interactions between risedronate and the metal ions, which also caused a decrease of the degrees of freedom of the resulting system.

Risedronate has higher $pL_{0.5}$ values at pH > 6.0 than similar chelating ligands such as methylglycindiacetate acid and phytate indicating that risedronate is a better sequestering agent in these conditions.

Further measurements to assess the nature and the solubility of the insoluble species are required, Setschenow coefficients for the neutral M_2L species have been provided in this work.

The availability of systematic studies on solution data regarding the interaction of bisphosphonates with metal cations is still scarce, however these data are useful to predict the bioavailability and the mechanism of action of risedronate in the presence of metal cations and to realize other possible applications of this molecule. For example, due to their high stability constants with metal cations the possible use of risedronate complexes for remediation and imaging purposes could also be hypothesized.

Funding

We thank MIUR (Ministero dell'Istruzione, dell'Università e della Ricerca) for financial support (cofounded PRIN project with Prot. 2015MP34H3) and UniME (Research & Mobility2017, Prot. 009041).

Author Contributions

Conceptualization, Alberto Pettignano, Carmelo Sgarlata, Gabriele Lando and Silvio Sammartano; Formal analysis, Clemente Bretti, Salvatore Cataldo and Giuseppa Grasso; Funding acquisition, Concetta De Stefano, Paola Cardiano and Giuseppe Arena; Investigation, Clemente Bretti, Salvatore Cataldo and Giuseppa Grasso; Methodology, Concetta De Stefano, Giuseppe Arena, Gabriele Lando and Silvio Sammartano; Project administration, Alberto Pettignano, Carmelo Sgarlata and Gabriele Lando; Software, Concetta De Stefano, Giuseppe Arena, Carmelo Sgarlata and Silvio Sammartano; Supervision, Concetta De Stefano, Giuseppe Arena and Silvio Sammartano; Writing – original draft, Paola Cardiano, Alberto Pettignano, Carmelo Sgarlata and Gabriele Lando; Writing – review & editing, Paola Cardiano, Giuseppe Arena and Gabriele Lando.

All authors have read and agreed to the final version of the manuscript.

Data Availability Statement: Experimental data are available upon contacting G.L.

Conflicts of Interest: The authors declare no conflicts of interest.

References

[1] L.E. Cole, T. Vargo-Gogola, R.K. Roeder, Targeted delivery to bone and mineral deposits using bisphosphonate ligands, Adv. Drug Deliv. Rev. 99 (2016) 12.

[2] E.J. Carbone, K. Rajpura, B.N. Allene, E. Cheng, B.D. Ulery, K.W.H. Lo, Osteotropic nanoscale drug delivery systems based on small molecule bone-targeting moieties, Nanomed.-Nanotechnol. 13 (2017) 37.

[3] A. Bigi, E. Boanini, Calcium Phosphates as Delivery Systems for Biphosphonates, J. Funct. Biomater. 9 (2018) 6.

[4] G. Chindamo, S. Sapino, E. Peira, D. Chirio, M.C. Gonzalez, M. Gallarate, Bone Diseases: Current Approach and Future Perspectives in Drug Delivery Systems for Bone Targeted Therapeutics, Nanomaterials 10 (2020) 875.

[5] H.A. Fleisch, Bisphosphonates: Preclinical Aspects and Use in Osteoporosis, Ann. Med. 29 (1997) 55.

[6] S.A. Lloyd, S.E. Morony, V.L. Ferguson, S.J. Simske, L.S. Stodieck, K.S. Warmington, E.W. Livingston, D.L. Lacey, P.J. Kostenuik, T.A. Bateman, Osteoprotegerin is an effective countermeasure for spaceflight-induced bone loss in mice, Bone 81 (2015) 562.

[7] A.C.C. Chou, A.C.M. Ng, M.A. Png, D.T.C. Chua, D.C.E. Ng, T.S. Howe, J.S.B. Koh, Bone cross-sectional geometry is not associated with atypical femoral fractures in Asian female chronic bisphosphonate users, Bone 79 (2015) 170.

[8] T.J. Lin, Predicting binding affinities of nitrogen-containing bisphosphonates on hydroxyapatite surface by molecular dynamics, Chem. Phys. Lett. 716 (2019) 83.

[9] G.H. Nancollas, R. Tang, R.J. Phipps, Z. Henneman, S. Gulde, W. Wu, A. Mangood, R.G.G. Russell, E.F. H., Novel insights into actions of bisphosphonates on bone: differences in interactions with hydroxyapatite, Bone 38 (2006) 617.
[10] P. Tassone, P. Tagliaferri, C. Viscomi, C. Palmieri, M. Caraglia, A. D'Alessandro, A. Galea, A. Goel, A. Abbruzzese, C.R. Boland, S. Venuta, Zoledronic acid induces antiproliferative and apoptotic effects in human pancreatic cancer cells in vitro, Br. J. Cancer 88 (2003) 1971.
[11] B. Hofstetter, S. Gamsjaeger, R.J. Phipps, R.R. Recker, F.H. Ebetino, K. Klaushofer, E.P. Paschalis, Effects of alendronate and risedronate on bone material properties in actively forming trabecular bone surfaces, J. Bone Miner. Res. 27 (2012) 995.
[12] C. Prasad, S.L. Greenspan, K.T. Vujevich, A. Brufsky, B.C. Lembersky, G.J. van Londen, R.C. Jankowitz, S.L. Puhalla, P. Rastogi, S. Perera, Risedronate may preserve bone microarchitecture in breast cancer survivors on aromatase inhibitors: A randomized, controlled clinical trial, Bone 90 (2016) 123.
[13] C. Love, A.S. Din, M.B. Tomas, T.P. Kalapparambath, C.J. Palestro, Radionuclide bone imaging: an illustrative review, Radiographics 23 (2003) 341.
[14] J. Brüning, A.C. Petereit, E. Alig, M. Bolte, J.B. Dressman, M.U. Schmidt, Characterization of a new solvate of risedronate, J. Pharma. Sci. 100 (2011) 863.
[15] M. Malavasi, R. Louro, M.B. Barros, L.N. Teixeira, D.C. Peruzzo, J.C. Joly, E.F. Martinez, M.H. Napimoga, Effects of risedronate on osteoblastic cell cultures, Arch. Oral Biol. 68 (2016) 43.
[16] F. Errassifi, S. Sarda, A. Barroug, A. Legrouri, H. Sfihi, C. Rey, Infrared, Raman and NMR investigations of risedronate adsorption on nanocrystalline apatites, J. Colloid Interf. Sci. 420 (2014) 101.
[17] S. Mukherjee, C. Huang, F. Guerra, K. Wang, E. Oldfield, Thermodynamics of Bisphosphonates Binding to Human Bone: A Two-Site Model, J. Am. Chem. Soc. 131 (2009) 8374.
[18] M.S. Ironside, M.J. Duer, S.B. S., Bisphosphonate protonation states, conformations, and dynamics on bone mineral probed by solid-state NMR without isotope enrichment, Eur. J. Pharm. Biopharm. 76 (2010) 120.
[19] G.B. Deacon, C.M. Forsyth, N.B. Greenhill, P.C. Junk, J. Wang, Coordination Polymers of Increasing Complexity Derived from Alkali Metal Cations and (4-Amino-1-hydroxybutylidine)-1,1-bisphosphonic Acid (Alendronic Acid): The Competitive Influences of Coordination and Supramolecular Interactions, Cryst. Growth Des. 15 (2015) 4646.
[20] A.M. Hounslow, J. Carran, R.J. Brown, D. Rejman, G.M. Blackburn, D.J. Watts, Determination of the Microscopic Equilibrium Dissociation Costants for Risedronate and Its Analogues Reveals Two Distinct Roles for the Nitrogen Atom in Nitrogen- Containing Bisphosphonate Drugs, J. Med. Chem. 51 (2008) 4170.
[21] A. Itoh, Y. Akagi, H. Shimomura, T. Aoyama, Interaction between Bisphosphonates and Mineral Water: Study of Oral Risedronate Absorption in Rats, Biol. Pharm. Bull. 39 (2016) 323.
[22] E. Matczak-Jon, V. Videnova-Adrabińska, Supramolecular chemistry and complexation abilities of diphosphonic acids, Coord. Chem. Rev. 249 (2005) 2458.
[23] C. Foti, O. Giuffrè, S. Sammartano, Thermodynamics of HEDPA protonation in different media and complex formation with Mg^{2+} and Ca^{2+}, J. Chem. Thermodyn. 66 (2013) 151.
[24] C. Sgarlata, V. Zito, G. Arena, Conditions for calibration of an isothermal titration calorimeter using chemical reactions, Anal. Bioanal. Chem. 405 (2012) 1085.
[25] C. De Stefano, P. Princi, C. Rigano, S. Sammartano, Computer Analysis of Equilibrium Data in Solution. ESAB2M: An Improved Version of the ESAB Program, Ann. Chim. (Rome) 77 (1987) 643.
[26] C. De Stefano, S. Sammartano, P. Mineo, C. Rigano, in: A. Gianguzza, E. Pelizzetti, S. Sammartano (Eds.), Marine Chemistry - An Environmental Analytical Chemistry Approach, Kluwer Academic Publishers, Amsterdam, 1997, p. 71-83.
[27] G. Arena, P. Gans, C. Sgarlata, HypCal, a general-purpose computer program for the determination of standard reaction enthalpy and binding constant values by means of calorimetry, Anal. Bioanal. Chem. 408 (2016) 6413.
[28] L. Alderighi, P. Gans, A. Ienco, D. Peters, A. Sabatini, A. Vacca, Hyperquad simulation and speciation (HySS): a utility program for the investigation of equilibria involving soluble and partially soluble species, Coord. Chem. Rev. 194 (1999) 311.
[29] C. De Stefano, C. Foti, S. Sammartano, A. Gianguzza, C. Rigano, Equilibrium Studies in Natural Fluids. Use of Synthetic Seawater and Other Media as Background Salts, Ann. Chim. (Rome) 84 (1994) 159.
[30] J.N. Brönsted, Studies on solubility IV. Principle of the specific interaction of ions, J. Am. Chem. Soc. 44 (1922) 887.
[31] L. Ciavatta, The specific interaction theory in the evaluating ionic equilibria, Ann. Chim. (Rome) 70 (1980) 551.

[32] I. Grenthe, I. Puigdomenech, Modelling in aquatic chemistry. OECD-NEA, Paris, France, 1997.
[33] E.A. Guggenheim, J.C. Turgeon, Specific interaction of ions, Trans. Faraday Soc. 51 (1955) 747.
[34] G. Scatchard, Concentated solutions of strong electrolytes, Chem. Rev. 19 (1936) 309.
[35] C. Bretti, R.M. Cigala, C. De Stefano, G. Lando, S. Sammartano, Understanding the bioavailability and sequestration of different metal cations in the presence of a biodegradable chelant S,S-EDDS in biological fluids and natural waters, Chemosphere 150 (2016) 341.
[36] F. Crea, C. De Stefano, C. Foti, D. Milea, S. Sammartano, Chelating agents for the sequestration of mercury(II) and monomethyl mercury(II), Curr. Med. Chem. 21 (2014) 3819.
[37] C. Bretti, S. Cataldo, R.M. Cigala, G. Lando, A. Pettignano, S. Sammartano, Understanding the Bioavailability of Ca2+ in Biological Fluids in the Presence of Risedronic Acid, SM J. Bioequiv. Availab. 1 (2017) 1001.
[38] C. Bretti, I. Cukrowski, C. De Stefano, G. Lando, Solubility, Activity Coefficients and Protonation Sequence of Risedronic Acid, J. Chem. Eng. Data 59 (2014) 3728.
[39] C. Bretti, C. De Stefano, G. Lando, K. Majlesi, S. Sammartano, Thermodynamics (Solubility and Protonation Constants) of Risedronic Acid in Different Media and Temperatures (283.15–318.15 K), J. Solution Chem. 46 (2017) 1903.
[40] C. Ekberg, P.L. Brown, Wiley-VCH Verlag GmbH & Co. KGaA, Boschstr, Weinheim, Germany, 2016.
[41] S. Cataldo, S. Orecchio, G. Lando, D. Milea, A. Pettignano, S. Sammartano, A novel thermodynamic approach for the complexation study of toxic metal cations by a landfill leachate, New. J. Chem. 42 (2018) 7640.
[42] E. Matczak-Jon, B. Kurzak, A. Kamecka, P. Kafarskic, Interactions of zinc(II), magnesium(II) and calcium(II) with aminomethane-1,1-diphosphonic acids in aqueous solutions, Polyhedron 21 (2002) 321.
[43] A.E. Martell, R.M. Smith, R.J. Motekaitis, NIST Standard Reference Database 46, vers.8. Gaithersburg, 2004.
[44] X. Fang, S. Zhu, J. Ma, F. Wang, H. Xu, M. Xia, The facile synthesis of zoledronate functionalized hydroxyapatite amorphous hybrid nanobiomaterial and its excellent removal performance on Pb^{2+} and Cu^{2+}, J. Haz. Mat. 392 (2020) 122291.
[45] C. Bretti, R.M. Cigala, C. De Stefano, G. Lando, S. Sammartano, Understanding the bioavailability and sequestration of different metal cations in the presence of a biodegradable chelant MGDA in biological fluids and natural waters, Chemosphere 183 (2017) 107.
[46] R.M. Cigala, F. Crea, C. De Stefano, G. Lando, D. Milea, S. Sammartano, Electrochemical Study on the Stability of Phytate Complexes with Cu^{2+}, Pb^{2+}, Zn^{2+}, and Ni^{2+}: A Comparison of Different Techniques, J. Chem. Eng. Data 55 (2010) 4757.
[47] C. Bretti, C. Foti, N. Porcino, S. Sammartano, SIT parameters for 1:1 electrolytes and correlation with Pitzer coefficients, J. Solution Chem. 35 (2006) 1401.